



Pharmacokinetics, mass balance, tissue distribution, metabolism, and excretion of pralicyguat, a clinical-stage soluble guanylate cyclase stimulator in rats

Ali R. Banijamali | Andrew E. Carvalho | James D. Wakefield | Peter Germano  | Timothy C. Barden | Jenny V. Tobin | Daniel P. Zimmer | Jaime L. Masferrer | Albert T. Profy | Mark G. Currie | G. Todd Milne

Department of Drug Metabolism and Pharmacokinetics, Cycleron Therapeutics, Cambridge, MA, USA

Correspondence

Peter Germano, Department of Drug Metabolism and Pharmacokinetics, Cycleron Therapeutics, 301 Binney Street, Cambridge, MA 02142.
Email: pgermano@cycleron.com

Abstract

The pharmacokinetics (PK), metabolism, excretion, mass balance, and tissue distribution of [¹⁴C]pralicyguat were evaluated following oral administration of a 3-mg/kg dose in Sprague-Dawley rats and in a quantitative whole-body autoradiography (QWBA) study conducted in male Long-Evans rats. Plasma T_{max} was 1 hour and the $t_{1/2}$ of total plasma radioactivity was 23.7 hours. Unchanged pralicyguat accounted for 87.4%, and a minor metabolite (*N*-dealkylated-pralicyguat) accounted for 7.6% of the total radioactivity in plasma through 48 hours (AUC_{0-48}). Tissues with the highest exposure ratios relative to plasma were liver, intestines, adrenal gland, and adipose, and those with the lowest values were seminal vesicle, blood, CNS tissues, lens of the eye, and bone. Most of the [¹⁴C]pralicyguat-derived radioactivity was excreted within 48 hours after oral administration. Mean cumulative recovery of the administered radioactivity in urine and feces over 168 hours was 3.7% and 95.7%, respectively. Unchanged pralicyguat was not quantifiable in urine or bile of cannulated rats; however, based on the total radioactivity in these fluids, a minimum of approximately 82% of the orally administered dose was absorbed. [¹⁴C]Pralicyguat was metabolized via oxidative and glucuronidation pathways and the most abundant metabolites recovered in bile were pralicyguat-glucuronide and hydroxy-pralicyguat-glucuronide. These results indicate that pralicyguat had rapid absorption, high bioavailability, extensive tissue distribution, and elimination primarily via hepatic metabolism.

KEYWORDS

absorption, cGMP, excretion, mass balance, metabolism, nitric oxide, pharmacokinetics, pralicyguat, QWBA, sGC

Abbreviations: ACN, acetonitrile; AUC, area under the concentration-time curve; AUC_{all} , area under the concentration-time curve of all observed points; AUC_{inf} , area under the concentration-time curve extrapolated to infinity; BDC, bile duct cannulated; BQL, below quantitation limit; C_{max} , maximal concentration; HPLC, high-performance liquid chromatography; LC, liquid chromatography; LE, Long-Evans; LSC, liquid scintillation counting; M, metabolite number; MeOH, methanol; MS, mass spectrometry; NMR, nuclear magnetic resonance spectroscopy; NO, nitric oxide; PEG, polyethylene glycol; PK, pharmacokinetic; QWBA, quantitative whole-body autoradiography; SD, Sprague-Dawley; sGC, soluble guanylate cyclase; $t_{1/2}$, elimination half-lives; T_{last} , time of last measurable concentration; T_{max} , time to maximal concentration.

This is an open access article under the terms of the Creative Commons Attribution-NonCommercial-NoDerivs License, which permits use and distribution in any medium, provided the original work is properly cited, the use is non-commercial and no modifications or adaptations are made.

© 2020 The Authors. *Pharmacology Research & Perspectives* published by British Pharmacological Society and American Society for Pharmacology and Experimental Therapeutics and John Wiley & Sons Ltd

1 | INTRODUCTION

Praliguat (IW-1973) is a soluble guanylate cyclase (sGC) stimulator under development for the treatment of diabetic nephropathy (DN; ClinicalTrials.gov Identifier NCT03217591) and heart failure with preserved ejection fraction (HFpEF; ClinicalTrials.gov Identifier NCT03254485). sGC is a receptor for nitric oxide (NO) and plays a central physiological role in regulating blood flow, inflammation, and fibrosis.^{1,2} Upon binding NO, sGC catalyzes the conversion of guanosine-5'-triphosphate (GTP) to the second messenger cyclic guanosine-3',5'-monophosphate (cGMP) which in turn regulates multiple physiological processes.³ Praliguat is an allosteric modulator that binds to sGC and acts synergistically with NO to increase production of cGMP and amplify downstream signaling.

sGC stimulation has potential for the treatment of diseases where disruption of the NO-sGC-cGMP pathway has been implicated.⁴ Indeed, the sGC stimulator riociguat is approved for treatment of two forms of pulmonary hypertension.^{5,6} In addition, multiple sGC stimulators are in clinical development for a broad range of diseases. In particular, DN and HFpEF were chosen as indications for praliguat based on efficacy in multiple preclinical models of cardiovascular and renal disease.

For example, in a Dahl salt-sensitive rat model of hypertension and organ damage, praliguat-treated animals had lower blood pressure and lower levels of inflammatory cytokines and markers of renal disease, including proteinuria and renal fibrotic gene expression.⁷ Notable renoprotective effects were also observed in a rat unilateral ureteral obstruction renal fibrosis model, wherein treatment with praliguat for 14 days following ureteral obstruction resulted in reductions in markers of renal fibrosis. In addition, praliguat treatment in a lipopolysaccharide-induced inflammation study in mice demonstrated significant reductions in the pro-inflammatory cytokines IL-6 and TNF- α .⁷ Clinically, oral administration of praliguat in healthy volunteers was associated with elevation of cGMP and modest reductions in blood pressure, indicating target engagement and stimulation of the NO-sGC-cGMP pathway.⁸ These hemodynamic effects were also observed in an exploratory clinical study in patients with type 2 diabetes and hypertension, along with additional positive trends on metabolic and lipid parameters.⁹

Praliguat has a large volume of distribution in both preclinical and clinical studies, consistent with extensive distribution to tissues.^{7,8} Higher levels of drug in tissues than in the bloodstream could enhance sGC pharmacology in target organs while minimizing effects on systemic blood pressure. The purpose of this work was to characterize the pharmacokinetics, distribution, metabolism, and excretion of praliguat in rats.

2 | MATERIALS AND METHODS

2.1 | Chemicals

Praliguat (1,1,1,3,3,3-hexafluoro-2-(((5-fluoro-2-(1-(2-fluorobenzyl)-5-(isoxazol-3-yl)-1H-pyrazol-3-yl)pyrimidin-4-yl)amino)methyl)propan-2-ol) was synthesized at Cycleron Therapeutics at >99% chemical

purity. [¹⁴C]praliguat, uniformly labeled with carbon-14 on the phenyl ring with a specific activity of 75 mCi/mmol and radiochemical purity of >99%, was synthesized at American Radiolabeled Chemicals. The reference metabolites N-dealkylated-praliguat and *para*-hydroxy-praliguat were synthesized at Cycleron Therapeutics and praliguat-glucuronide was prepared at Hypha Discovery. Structures were confirmed by MS and NMR analysis.

2.2 | Dose preparation

The oral dosing formulation was prepared by mixing the appropriate quantities of [¹⁴C]praliguat, unlabeled praliguat, and the vehicle (PEG 400 in water [60:40 v:v]). For the mass balance, excretion, and PK studies, the formulation was prepared at a target concentration of 0.75 mg/mL and a target radioactivity of 34.5 μ Ci/mL, for a final dose of 3 mg/kg (104 μ Ci/kg) using a volume of 4 mL/kg. For the QWBA study, the same formulation concentration and volume were used, but the target radioactivity concentration was 50 μ Ci/mL, which resulted in a final dose concentration of 3 mg/kg and 200 μ Ci/kg.

2.3 | Animal preparation and dosing

Male Sprague-Dawley (SD) rats included in mass balance, excretion, and PK studies were purchased from Envigo RMS, Inc. The pharmacokinetic group (Group 1) consisted of 15 SD rats while Group 2 (non-bile duct cannulated) and Group 3 (bile duct cannulated) each consisted of 3 SD rats. Eleven Male Long-Evans (LE) pigmented rats, widely used in QWBA studies and safety assessments to human, included in the QWBA study were purchased from Hilltop Lab Animals, Inc. Each animal was weighed, randomized, and assigned a permanent identification number. During the acclimation period (at least 2 days before study initiation), the animals were housed in individual, suspended, stainless steel wire mesh cages. During the test period, animals were housed as appropriate for sample collection (as described below). All animal housing and care conformed to the standards recommended by the *Guide for the Care and Use of Laboratory Animals* (Institute of Laboratory Animal Resources, 1996). Food (Certified Rodent Diet 5002; PMI Nutrition International) and water were provided ad libitum, except when animals were fasted overnight (at least 12 hours) before and through 4 hours after dose administration. Animals were allowed free access to water the entire time. The animal room was controlled to maintain a temperature of 20°C-26°C, a relative humidity of 50 \pm 20%, and a 12 hour light/12 hour dark cycle. As necessary, the 12 hour dark cycle was interrupted to accommodate study procedures.

Animals for collection of blood (PK rats) were individually housed in suspended, stainless steel, wire-mesh cages. Bile duct-cannulated (BDC) animals for collection of bile, urine, and feces were individually housed in Nalgene cages designed for the separation and collection of bile, urine, and feces. Non-bile duct-cannulated (NBDC) animals for collection of excreta were individually housed in Nalgene

cages designed for the separation and collection of urine and feces. Animals designated for the tissue distribution study (QWBA) were placed in individual plastic shoebox cages with raised wire flooring and bedding and housed in these cages throughout the study period.

The formulated [^{14}C]pralicigat was administered to rats from each group by oral gavage. The study design, group designations, number of animals, body weights, target dose level, target dose volume, and samples collected from each group are summarized in Table 1.

2.4 | Sample preparation and radioanalysis

2.4.1 | Radioactivity determination

Radioactivity in plasma, blood, urine, bile, feces, and carcasses were determined using a Packard Tri-Carb model 2910TR liquid scintillation counter (PerkinElmer). Aliquots of 50-100 μL from each sample were used for radioactivity determination in duplicate by adding 15 mL of Ultima Gold XR scintillation cocktail (PerkinElmer) and was counted for at least 5 minutes.

2.4.2 | Blood and plasma

Blood was mixed by inverting several times, and duplicate weighed aliquots were taken. Commercial solubilizing agent was added to digest each sample. Samples were incubated for at least 1 hour at approximately 60°C, 0.1 mol/L di-sodium EDTA was added to reduce foaming, and 30% hydrogen peroxide was added to remove the color. The samples were left overnight to allow any foaming to dissipate. Scintillation cocktail was added, and the samples were shaken

and analyzed by liquid scintillation counting (LSC). The remaining blood was centrifuged at approximately 15 000 $\times g$ for approximately 10 minutes at approximately 5°C. Duplicate weighed aliquots of the resulting plasma samples were analyzed by LSC.

2.4.3 | Urine, bile, cage wash, and cage rinse

Samples were mixed by shaking, and duplicate weighed aliquots were analyzed by LSC.

2.4.4 | Feces

A sufficient amount of solvent (acetonitrile: water, 20:80, v:v) was added to facilitate homogenization. Samples were homogenized, and duplicate weighed aliquots were digested in 1 N sodium hydroxide and analyzed by LSC.

2.4.5 | Bile Cannulas and Cage wipes

A sufficient amount of solvent (acetonitrile: water, 20:80, v:v) was added to cover each sample. Samples were extracted, mixed by gentle shaking, and duplicate weighed aliquots were analyzed by LSC.

2.4.6 | Carcasses

Each carcass was digested in a weighed amount of 1 N sodium hydroxide until dissolved. Ethanol was added, and the sample was

TABLE 1 Summary of [^{14}C]Pralicigat Study Designs. The group designations, number of animals, target dose level, and target dose volume were as follows

Study/group	Number of rats/strain	Body weight (g)	dose route	Dose level (mg/kg)	Dose level ($\mu\text{Ci}/\text{kg}$)	Dose volume (mL/kg)	Sample/collection time points (h)
Mass balance/1(PK)	15/SD	219-326	Oral	3	104	4	Blood: 0.25, 0.5, 1, 2, 4, 8, 12, 24, 48, 72, 120
Mass balance/2 (NBDC)	3/SD	219-326	Oral	3	104	4	Urine: 0-8, 8-24, 24-48, 48-72, 72-96, 96-120, 120-144, 144-168 Feces: 0-24, 24-48, 48-72, 72-96, 96-120, 120-144, 144-168 Carcass: 0-168
Mass balance/3 (BDC)	3/SD	219-326	Oral	3	104	4	Bile & Urine: 0-4, 4-8, 8-24, 24-48, 48-72, 72-96, 96-120 Feces: 0-24, 24-48, 48-72, 72-96, 96-120, 120-144, 144-168 Carcass: 0-120
Tissue distribution (QWBA)	11/LE	203-276	Oral	3	200	4	Carcass: 1, 2, 4, 8, 12, 24, 48, 72, 96, 168, 504

Abbreviations: BDC, Bile duct cannulated; LE, Long-Evans; NBDC, Non-bile duct cannulated (intact rats); PK, pharmacokinetics; QWBA, quantitative whole-body autoradiography; SD, Sprague-Dawley.

homogenized by mixing. Duplicate weighed aliquots were analyzed by LSC.

2.4.7 | Quantitative whole-body autoradiography

QWBA assays were performed as described by Solon & Lee.¹⁰ In brief, each frozen rat carcass was embedded in a 2% carboxymethylcellulose matrix with a microtome stage at -20°C . Three quality control standards of [^{14}C]glucose at 0.05 $\mu\text{Ci/g}$ were placed into the frozen blocks before sectioning and were used for section thickness quality control. Several 40- μm sections at various levels in the whole body were collected to include the major tissues, organs, and biological fluids; the whole-body sections were dried in a cryomicrotome at -20°C for at least 48 hours. Sections were mounted on a cardboard backing, covered with a thin plastic wrap, and exposed along with calibration standards of [^{14}C]glucose at 10 different concentrations (0.0009595 to 7.806 $\mu\text{Ci/g}$) to a ^{14}C -sensitive phosphor imaging plate (Fuji Biomedical). The imaging plates and sections were kept in a copper-lined lead radiation safe chamber for a 4-day exposure at room temperature. After exposure, the imaging plates were scanned using the Typhoon 9410 image acquisition system (GE/Molecular Dynamics), and the whole-body images were stored in a computer. Radioactivity concentration of tissues was quantified by image densitometry using MCID image analysis software. Tissue concentration data were obtained for adipose (brown and white), adrenal gland, aorta, vena cava, bile (in duct), blood (cardiac), bone, bone marrow, brain (cerebrum, cerebellum, hippocampus, medulla), cecum (and contents), epididymis, esophagus, eye (uvea and lens), Harderian gland, heart, kidney (cortex and medulla), large intestine (and contents), liver, lung, lymph node, mammary gland region, oral mucosa, pancreas, penis, pituitary gland, prostate gland, salivary gland, seminal vesicles, skeletal muscle, skin [pigmented and nonpigmented, small intestine (and contents)], stomach (gastric mucosa and contents), spleen, spinal cord, testis, thymus, thyroid, and urinary bladder (and contents). The concentrations of radioactivity were expressed as the microgram equivalents of [^{14}C]praliguat per gram of sample. An upper and lower limit of quantification was applied to the data, determined by using the radioactive concentration of the highest and lowest calibration standards divided by the specific activity of the test article formulation.

2.4.8 | Plasma and tissue pharmacokinetic analysis

Nominal times were used for plasma and tissue PK calculations. Phoenix[®] WinNonlin[®], v. 6.3 (Pharsight Corporation) was used to determine noncompartmental PK parameters [Maximal concentration (C_{max}), Time of maximal concentration (T_{max}), Terminal half-life ($t_{1/2}$), Area under the curve extrapolated to infinity (AUC_{inf}), and area under the curve of all observed points (AUC_{all})]. The acceptance criteria for terminal half-life determination included regression of at least three time points in the elimination phase and a regression coefficient (r^2) $>.85$.

2.4.9 | Preparation of samples for metabolite profiling and identification

Equivalent amounts of plasma sample from Group 1 (PK) rats were pooled by time point. Samples were further pooled to generate a 0.5–48 hours AUC-representative pooled sample, including between 6 and 432 μL of each sample determined by using a time-weighted pooling method.¹¹ Pooled plasma samples were extracted with acetonitrile (ACN), sonicated, vortex mixed, and centrifuged. The supernatants were removed, and the extraction was repeated. The respective ACN supernatants were combined and evaporated to dryness under nitrogen. Residues were reconstituted in 90:10 (v/v) water:ACN, sonicated, vortex mixed, and centrifuged.

Urine samples were pooled at 4- to 24-hour intervals by group (equivalent % by weight) from collections of up to 120 hours for Group 3 (BDC) and up to 168 hours for Group 2 (NBDC). Pooled urine samples were centrifuged prior to analysis.

Bile samples from Group 3 rats were pooled (equivalent % by weight) at 4- to 24-hour intervals from collections up to 120 hours. Pooled bile samples were centrifuged prior to analysis.

Fecal samples collected from Group 2 and Group 3 rats were pooled at 24-hour intervals by group (equivalent % by weight) from collections of up to 120 hours for Group 3 (BDC) and up to 168 hours for Group 2 (NBDC). Aliquots of each sample were digested in 1 N sodium hydroxide and analyzed by LSC to determine the concentrations of radioactivity. Pooled feces samples were extracted with ACN, sonicated, vortex mixed, and centrifuged. The supernatants were removed, and the extraction was repeated. The respective ACN supernatants were combined and analyzed by LSC. Supernatants were then evaporated to dryness under nitrogen, reconstituted in MeOH, sonicated, vortex mixed, and centrifuged prior to analysis.

2.4.10 | Metabolite profiling and identification

Metabolite profiling and identification was conducted for the plasma, urine, bile, and feces using an HPLC-radiochromatography-MS system. The HPLC system was an Acquity I-Class binary solvent manager system (Waters) equipped with an Acquity sample manager FTN autoinjector, a UV detector, and a Phenomenex, Kinetex XB-C18, 4.6 \times 250 mm, 5 μm column, and a Phenomenex, KrudKatcher Ultra guard column. The mobile phase consisted of two solvents: solvent A, 0.1% (v/v) formic acid in water; and solvent B, 0.1% (v/v) formic acid in ACN. The gradient used was as follows: solvent B started at 10% hold for 1.5 minutes, linearly increased to 90% over 50 minutes, increased to 95% at 50.1 minute, held at 95% for 4.9 minutes, and then decreased to 10% at 55.1 minutes. The HPLC effluent (1 mL/min) was collected into Deepwell LumaPlate-96 plates containing solid scintillant (PerkinElmer Life and Analytical Sciences) at 10-second intervals. The plates were dried with a Savant Speed-Vac System (Global Medical Instrumentation) and counted for 10 min/well with a TopCount

analyzer (PerkinElmer Life and Analytical Sciences). Radioactivity in each well was determined using TopCount analysis, and radiochemical profiles were generated based on radioactivity counts. Radioactivity profiles were prepared by plotting the resulting net counts per minute values vs HPLC time and radiochromatograms were reconstructed from the TopCount data using Microsoft Excel 2016 software. Mass spectral analysis was performed on a Vion IMS Q-TOF mass spectrometer (Waters) operated in positive ion electrospray mode using the HPLC and chromatography conditions as described above.

3 | RESULTS

3.1 | Mass balance study

Following oral administration to SD rats (PK, Group 1), the highest mean concentrations (C_{max}) of radioactivity in blood and plasma

TABLE 2 Radioactive dose recovered in urine, feces, bile, cage rinses, and carcass at specified intervals after a single oral administration of [14 C]praliguat to non-bile duct cannulated (NBDC) and bile duct cannulated (BDC) rats, expressed as percent administered dose (%AD)

Time point (h)	NBDC (group 2)		BDC (group 3)		
	Urine	Feces	Urine	Feces	Bile
0-24	2.59	31.7	1.72	7.11	50.8
24-48	0.718	42.3	0.463	2.96	17.3
48-72	0.227	13.8	0.136	0.912	6.87
72-96	0.097	4.62	0.048	0.428	3.23
96-120	0.045	1.83	0.022	0.369	1.76
120-144	0.022	0.966	-	-	-
144-168	0.016	0.448	-	-	-
Subtotal	3.72	95.7	2.39	11.8	80
Cage Rinse	1.05		0.44		
Carcasses	0.83		2.92		
Total Recovery	101		97.6		

Note: % AD values are given as the mean of the duplicate weighed aliquots (pooled by time point).

TABLE 3 Pharmacokinetic parameters for [14 C]praliguat-derived radioactivity in the circulation

Study	Matrix	C_{max} (ng Eq/g)	T_{max} (h)	T_{last} (h)	AUC_{last} (ng Eq-h/g)	AUC_{inf} (ng Eq-h/g)	$t_{1/2}$ (h)
Mass balance (group 1) ^a	Plasma	371	1	72	4980	5050	12.5
	Blood	301	1	120	5300	5800	42.8
QWBA ^b	Plasma	293	1	96	2750	2850	23.7
	Blood (cardiac)	245	1	72	3200	3770	26.7

Note: Eq, Equivalents [14 C]praliguat.

^aPharmacokinetic (PK) parameters were calculated by noncompartmental analysis using sparse sampling.

^bOne rat was used per time point.

were 301 and 371 ng Eq [14 C]praliguat/g, respectively, observed at 1 hour postdose (T_{max}). The concentrations of radioactivity in blood and plasma then declined steadily and the elimination half-lives ($t_{1/2}$) for total radioactivity were 42.8 and 12.5 hours in blood and plasma, respectively.

After single oral doses of [14 C]praliguat to intact rats (NBDC, Group 2), approximately 77% of the radioactive dose was recovered in urine and feces through 48 hours (Table 2), indicating rapid elimination of the compound. The mean % administered radioactivity excreted was 3.7 and 95.7% for urine and feces, respectively, by 168 hours postdose. Peak urinary and fecal elimination of radioactivity occurred 0-24 hour postdose. The overall mean recovery of radioactivity following oral dosing to intact rats was 101% (Table 2). Unchanged praliguat accounted for less than 7% of the radioactive dose in feces and was below the limit of quantitation in urine.

After single oral doses of [14 C]praliguat to BDC rats (Group 3), mean recovery of total radioactivity in rat bile, urine, and feces over the 0-120 hours collection period was 97.6%. Biliary excretion accounted for 80% of the radioactive dose. Fecal and urinary excretion accounted for 11.8% and 2.4% of the radioactive dose, respectively (Table 2). Peak biliary excretion of radioactivity occurred between 8 and 24 hours postdose. Based on the total radioactivity excreted in urine and bile after oral administration, a minimum of approximately 82% of the orally administered dose was absorbed. Unchanged [14 C]praliguat was not quantifiable in bile and urine, and in feces accounted for about 6% of the administered dose.

3.2 | QWBA

After single oral doses of [14 C]praliguat to pigmented rats (LE), the distribution of radioactivity was determined using QWBA and the mean PK parameters for [14 C]praliguat-derived radioactivity are reported in Table 3 (plasma and cardiac blood) and Table 4 (tissues). The C_{max} in blood and plasma was 245 and 293 ng Eq/g at a T_{max} of 1 h, and the $t_{1/2}$ was 26.7 and 23.7 hours, respectively.

Plasma and tissue concentration-vs-time profiles for pigmented rats are illustrated in Figure 1. Whole-body autoradiograms showing patterns of radioactivity distribution in tissues are illustrated in Figure 2. The [14 C]praliguat-derived radioactivity was widely distributed and 19 of 40 tissues had concentrations that were higher

Matrix	$t_{1/2}$ (h)	T_{max} (h)	C_{max} (μg equiv/g)	AUC_{All} (μg equiv-h/g)	AUC_{All} tissue:plasma ratio
Adipose (brown)	16	4	3.65	42.7	15
Adipose (white)	14.6	8	3.66	81.2	28.5
Adrenal Gland	32	1	10.1	85.9	30.1
Aorta	6.8	1	1.7	19.3	6.76
Blood (cardiac)	26.7	1	0.245	3.38	1.18
Bone (femur) ^a	(17.4 ^a)	4	0.14	1.13	0.4
Bone Marrow (femur)	22.6	1	2.18	13.7	4.8
Brain (cerebellum)	8.5	1	0.6	3.03	1.06
Brain (cerebrum)	9.2	1	0.66	3.01	1.05
Brain (hippocampus)	9.1	1	0.615	2.55	0.89
Brain (medulla)	9.2	1	0.646	2.91	1.02
Cecum	19.1	8	3.08	28.8	10.1
Epididymis	15.6	1	0.633	9.19	3.22
Esophagus	24.5	1	0.991	11.9	4.18
Eye (lens)	ND	8	0.034	0.342	0.12
Eye (uvea)	25.2	1	0.987	8.53	2.99
Harderian Gland	13.4	1	2.83	21.2	7.42
Heart	11.7	1	1.76	15.4	5.4
Kidney (cortex)	50.6	1	2.8	19	6.64
Kidney (medulla)	19.9	1	2.04	13.1	4.59
Large Intestine	7.4	1	1.53	49.8	17.5
Liver	71.9	8	15.5	492	172
Lung	25.8	1	1.19	9	3.15
Pancreas	14.8	1	2.63	12.5	4.39
Pituitary gland	10.6	1	1.9	9.68	3.39
Plasma (LSC)	23.7	1	0.293	2.86	1
Preputial gland	41.7	1	2.66	24.8	8.67
Prostate	21.2	1	0.908	6.69	2.34
Salivary Gland	18.6	1	2.68	16.7	5.84
Seminal vesicle	15	1	0.341	3.83	1.34
Skeletal muscle	11.1	1	0.922	4.73	1.66
Skin (pigmented)	18.4	1	0.709	11.9	4.16
Small intestine	25.2	4	52.9	356	125
Spinal cord	8.3	1	0.465	2.83	0.99
Spleen	41.7	1	1.8	12.3	4.3
Stomach (gastric mucosa)	21.7	4	3.54	32.4	11.4
Testis	15.8	1	0.55	7.39	2.59
Thymus	11.6	1	1.17	8.97	3.14
Thyroid	15.5	1	2.99	26	9.1
Vena Cava	6.3	1	1.48	8.65	3.03

TABLE 4 Pharmacokinetic parameters of radioactivity in tissues of male LE rats after a single oral dose of 3 mg/kg [¹⁴C] praliguat

Note: ND, Value could not be determined due to insufficient data. One rat was used per time point.

^aTreat the $t_{1/2}$ and $AUC_{inf,obs}$ values with caution because the r^2 value and/or the number of time points used in the regression line to determine $t_{1/2}$ did not meet acceptable criteria (ie, $r^2 < 0.85$ and/or the number of time points was < 3).

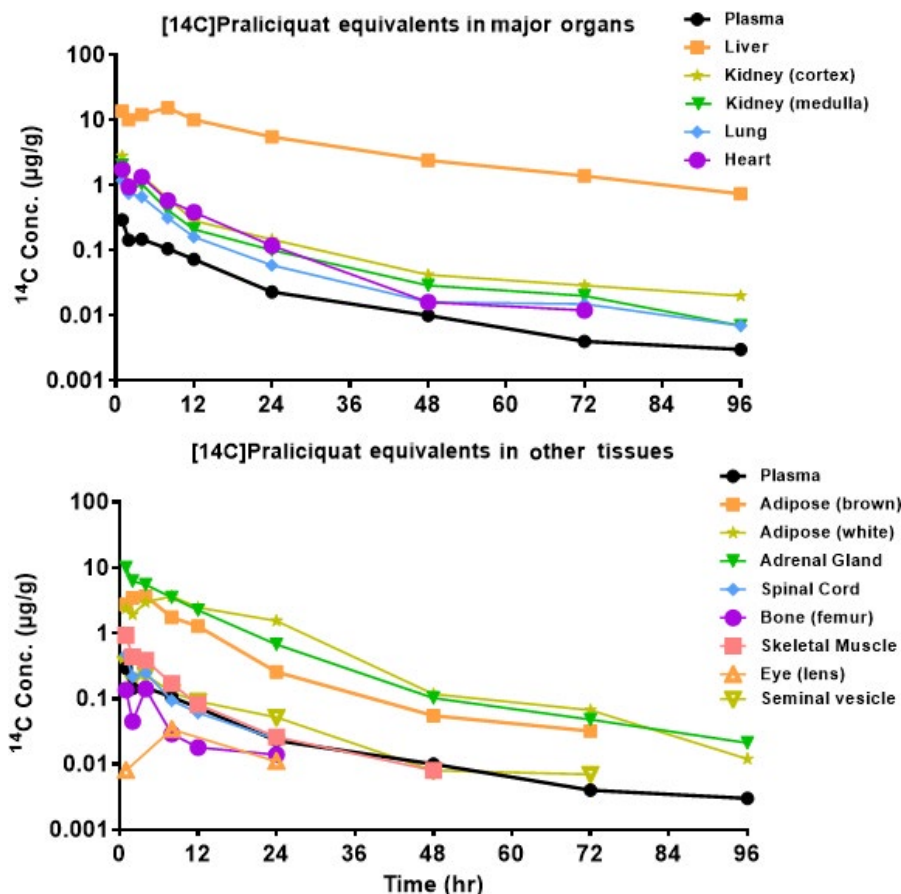
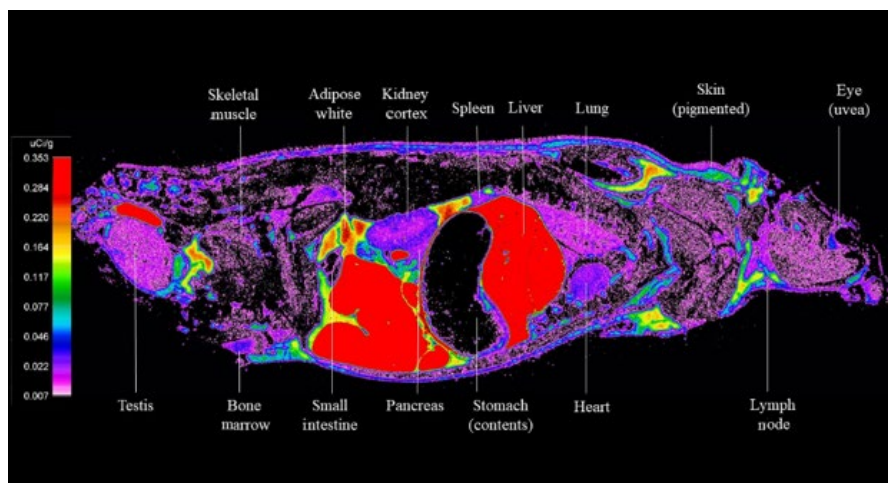


FIGURE 1 Tissue concentration-vs-time profiles for pigmented rats. The concentrations of radioactivity were expressed as the microgram equivalents of [¹⁴C]praliquat equivalents per gram of sample. One rat was used per time point

FIGURE 2 Whole-body autoradiogram of the radioactivity distribution in a male LE rat at 12 h following a single oral dose of [¹⁴C]praliquat. Concentration of praliquat expressed as equivalents per gram of tissue (µCi/g)

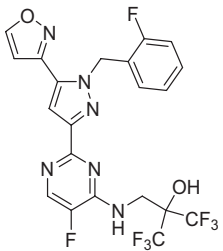
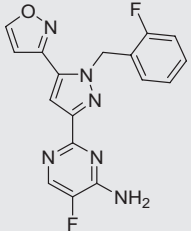
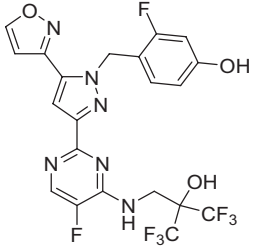
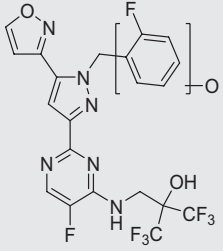
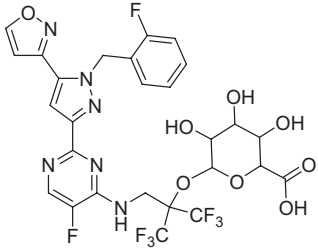
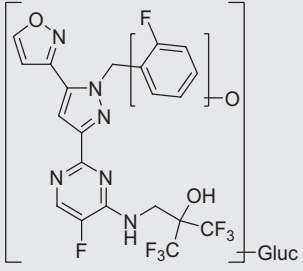


than in blood at all time points. The T_{max} of [¹⁴C]praliquat-derived radioactivity was found at 1 hours in most tissues (32 of 40, Table 4). Tissues exhibiting high concentrations ($C_{max} > 3.0 \mu\text{g Eq/g}$) were as follows: small intestine (52.9 $\mu\text{g Eq/g}$), liver (15.5 $\mu\text{g Eq/g}$), adrenal gland (10.1 $\mu\text{g Eq/g}$), white adipose (3.7 $\mu\text{g Eq/g}$), brown adipose (3.6 $\mu\text{g Eq/g}$), stomach (3.6 $\mu\text{g Eq/g}$), and cecum (3.1 $\mu\text{g Eq/g}$). The tissues exhibiting low concentrations ($C_{max} < 0.2 \mu\text{g Eq/g}$) were bone and pigmented eye lens. The highest overall concentrations were observed

in the contents of the alimentary canal (C_{max} ranged from 69.2 $\mu\text{g Eq/g}$ in cecum at 8 hours to 364.8 $\mu\text{g Eq/g}$ in stomach at 4 hours) and in bile (32.3 $\mu\text{g Eq/g}$ at 1 hours), which reflected the major routes of elimination for the [¹⁴C]praliquat-derived radioactivity after an oral dose. A relatively low concentration was observed in urine (1.1 $\mu\text{g Eq/g}$ at 8 hours).

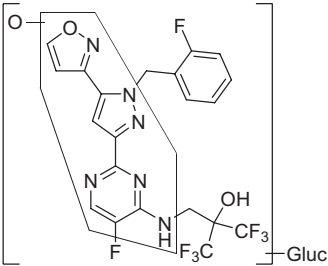
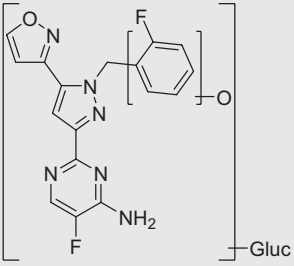
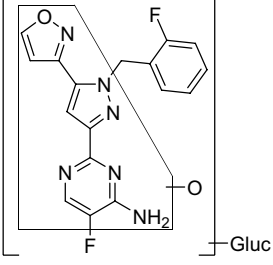
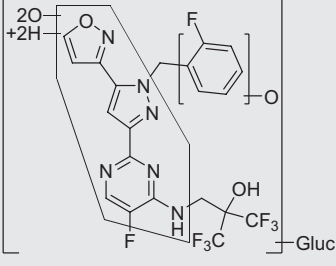
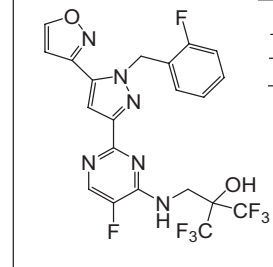
Concentrations in most tissues decreased steadily after T_{max} and were BQL in all tissues except liver at 504 hours postdose.

TABLE 5 Summary of protonated molecular ions and characteristic product ions for praliquat and identified metabolites

Metabolite designation	[M + H] ⁺	Proposed metabolite identification	Characteristic product ions (m/z)	Matrix
Praliquat	535		507, 439, 109, 83	Plasma Feces
M1	355		109	Plasma Bile Feces
M2A	551		427, 260, 125	Bile Feces
M2B	551		523, 439, 427, 125	Feces
M3	711		535, 507, 109	Urine Bile
M4A	727		551, 427, 125	Bile
M4B	727			
M4C	727			

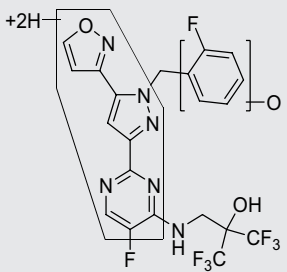
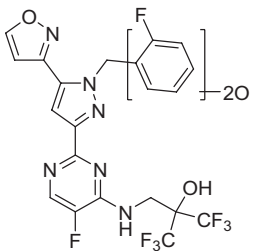
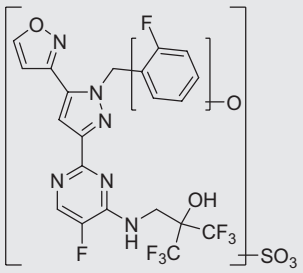
(Continues)

TABLE 5 (Continued)

Metabolite designation	[M + H] ⁺	Proposed metabolite identification	Characteristic product ions (m/z)	Matrix
M4D M4E M4F	727		551, 443, 109	Bile
M5A	547		247, 125	Bile
M5B M5C	547		371, 109	Bile
M6	761		461, 125	Bile
M7	858		840, 822, 711, 694, 567, 535, 427	Bile

(Continues)

TABLE 5 (Continued)

Metabolite designation	[M + H] ⁺	Proposed metabolite identification	Characteristic product ions (m/z)	Matrix
M8A	553		525, 508, 429, 401, 384, 125	Feces
M8B	553			
M9A	567		427, 141	Feces
M9B	567			
M10A	631		551, 427, 125	Bile
M10B	631			

Note: Values are representative.

Concentrations in the pigmented skin and in the pigmented eye were BQL by 96 hours and 168 hours, respectively. The tissues with the longest $t_{1/2}$ values were liver (71.9 hours), kidney cortex (50.6 hours), preputial gland and spleen (41.7 hours), and adrenal gland (32.0 hours); tissues with the shortest $t_{1/2}$ were aorta (6.8 hours), large intestine (7.4 hours), spinal cord (8.3 hours), and CNS tissues (range of 8.5-9.2 hours).

The AUCall blood-to-plasma exposure ratio was 1.18. Most tissues (29 of 40) had tissue-to-plasma exposure ratios that were >2.0 (Table 4). Tissues with the highest ratios were liver (172.4), small intestine (124.7), adrenal gland (30.1), white adipose (28.5), large intestine (17.5), brown adipose (15.0), stomach (11.4), and thyroid (9.1). Relatively high exposure ratios were also found in organs such as the heart (5.4), kidney (cortex 6.4, medulla 4.6), lung (3.2), and pancreas (4.4). The lowest exposure ratios were found in the seminal vesicle (1.34), tissues of the CNS (range 0.9-1.1), bone (0.4), and eye lens (0.1).

3.3 | Metabolite profiling/identification

Praliguat and its metabolites in plasma, urine, bile, and feces were identified using accurate mass measurements and +ESI LC/MS/MS analyses. A total of 21 metabolites were identified with a mass accuracy of <3.5 ppm. LC/MS/MS mass spectra revealed several characteristic

fragmentation patterns that allowed clear structural identification of the metabolites. Hydroxylation of praliguat resulted in formation of several regioisomeric hydroxy metabolites. The cut-off for identification of metabolites was 1% of the sample radioactivity for plasma and 1% of the administered radioactive dose. A summary of metabolites identified in plasma, urine, bile, and feces is presented in Table 5.

3.4 | Plasma

The HPLC radiochromatogram profile of pooled (1 hour) plasma samples contained two peaks (Figure 3) that were identified as praliguat and N-dealkylated-praliguat (M1) by comparison with reference standards and LC-MS analysis. Unchanged praliguat accounted for approximately 87% of the total radioactive exposure through 48 hour. N-dealkylated-praliguat was a minor circulating component contributing approximately 8% of the total radioactivity exposure (Table 6).

3.5 | Urine

Metabolite profiles in urine from BDC and NBDC rats showed six radioactive peaks, one of which was identified as praliguat-glucuronide

FIGURE 3 +ESI Extracted ion chromatogram (*m/z* 355.1113) of metabolite M1 and HPLC radiochromatogram from analysis of a 1-hour pooled plasma sample after a single oral dose of [¹⁴C]praliquat to Sprague-Dawley rats

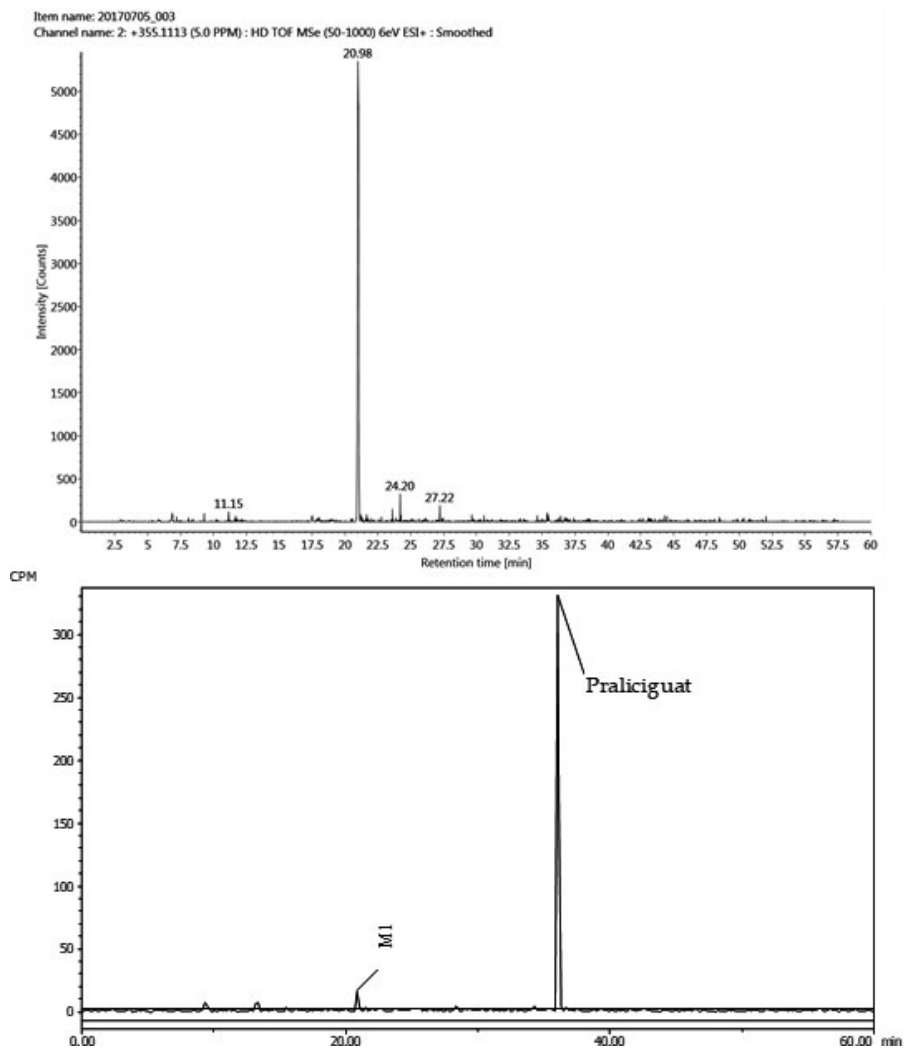


TABLE 6 Percent of sample radioactivity and concentrations of radioactivity as ¹⁴C praliquat or metabolites in pooled plasma samples after a single oral dose of ¹⁴C praliquat to male rats (Group 1, 3 mg/kg)

Metabolite designation	Retention time (minutes)	Collection time (Hours)					
		0.5	1	8	24	48	AUC
Percent of radioactivity injected (% of Run)							
M1	20.8	2.19	2.8	4.55	ND	ND	7.56
Praliquat	36	96.1	93.3	93.4	89.5	ND	87.4
	Total:	98.2	96.1	97.9	89.5	0	95
Concentration (ng equivalents/g)							
M1	20.8	5.01	9.37	7.44	ND	ND	7.18
Praliquat	36	220	312	153	41.5	ND	83
	ng equivalents/g quantitated:	225	322	160	41.5	0	90.2
	ng equivalents/g in sample:	285	371	180	56.6	19.3	97
	Extraction recovery (%):	100	100	100	83.2	59.5	100
	Reconstitution recovery (%):	80.3	90.2	90.9	98.4	100	97.9

Note: ND, Peak not detected or below the established limit of quantitation (1% of run and 10 cpm peak height).

(M3) by comparison with reference standard and by LC-MS analysis. No quantifiable unchanged praligicuat was recovered in urine. All the components detected in urine were each <0.1% of the administered dose.

3.6 | Bile

Praligicuat metabolite profiles in bile consisted of 13 radioactive peaks, and no unchanged praligicuat was recovered. Hydroxy-praligicuat-glucuronides (six regioisomers: M4A, M4B, M4C, M4D, M4E, and M4F) were collectively the most abundant metabolites in bile, accounting for a total of 20.2% of the administered dose. These metabolites are likely derived from glucuronidation of hydroxy-praligicuat regioisomers and/or from oxidation of praligicuat-glucuronide (M3), which was the most abundant single metabolite in bile and accounted for 11.3% of the administered dose. N-dealkylated-oxy-praligicuat-glucuronide/hydroxyl-praligicuat-glutathione conjugate (M5C/M7) and N-dealkylated-praligicuat (M1) were also significant metabolites identified in bile and accounted for 9.8 and 8.1% of the administered dose, respectively. Minor metabolites identified in bile were the result of N-dealkylation, hydroxylation, and glucuronidation of praligicuat (M5A and M5B), as well as hydroxylation and sulfate conjugation of praligicuat (M10A/M10B). Remaining components each generally accounted for <1% of the administered dose.

3.7 | Feces

Profiles in feces consisted of 12 radioactive peaks that were identified as unchanged praligicuat and its metabolites. Unchanged praligicuat was recovered in feces from both NBDC and BDC rats and accounted for 6.65 and 6.16% of the administered dose, respectively.

The majority of components detected in feces each accounted for <1% of the administered dose. Most of the metabolites detected in feces from NBDC rats were not detected in feces from BDC rats, likely due to bile collection. Dihydro-hydroxy-praligicuat (M8A and M8B) and hydroxy-praligicuat (M2A, M2B, and M2C) regioisomers were the most abundant metabolites in feces from NBDC rats, accounting for 7.99 and 10.5% of the administered dose, respectively.

3.8 | Pathway of metabolism

The metabolic pathway for praligicuat involved oxidation, reduction, dealkylation, sulfation, glucuronidation, and glutathione conjugation (Figure 4).

4 | DISCUSSION

The purpose of these studies was to investigate the ADME properties of praligicuat in male rats after single oral doses. The absorption and distribution of [14 C]praligicuat was rapid, producing similar C_{max} levels in SD and LE rats at a T_{max} of 1 hour in the plasma, blood, and most organs. Based on the total radioactivity excreted in urine and bile, at least 82% of the dose was absorbed.

The QWBA study revealed that praligicuat was widely distributed, which is consistent with the large volume of distribution found for praligicuat in pharmacological studies in the rat (V_{ss} 10.5 L/kg,⁷ and with the apparent volume of distribution in the humans (V_z/F 3100-3610 L, 8). Tissues with the highest exposure ratios relative to plasma were liver, intestines, adrenal gland, and adipose, and those with the lowest values were seminal vesicle, blood, CNS tissues, lens of the eye, and bone, there was no specific association with melanin in the skin or eye. These results

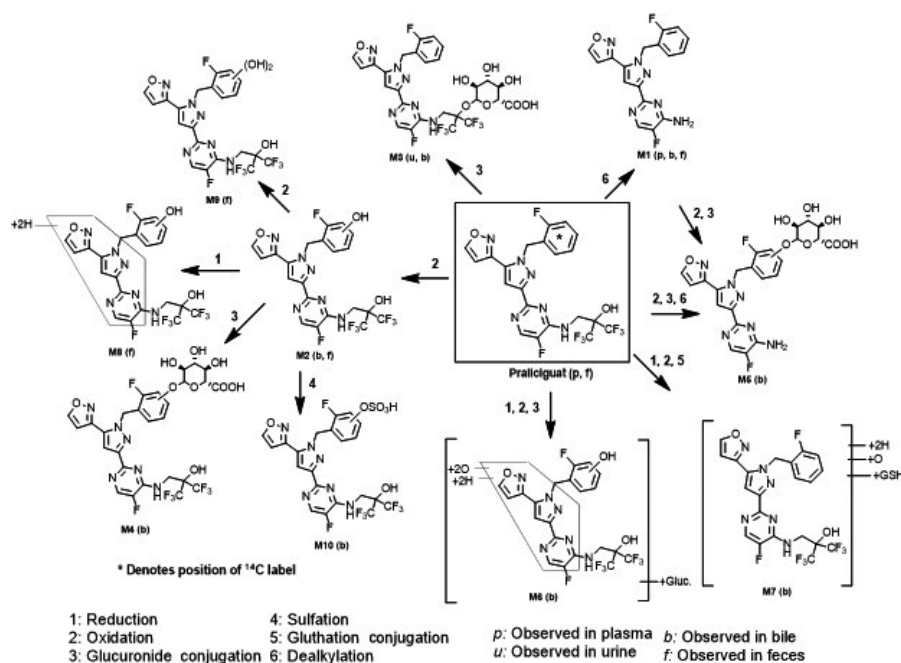


FIGURE 4 Proposed metabolic pathway for praligicuat in rats

indicate praligicuat levels are highest in fatty tissues, which is likely driven by the high lipophilicity of the compound ($\text{LogD}_{7.4}$ 3.66). Praligicuat's high lipophilicity and tissue distribution are also consistent with the biphasic plasma concentration-time profile, with dissipation rates in the nonclearance tissues generally reflecting the terminal elimination phase.

Metabolite profiling showed that the parent drug was the major component in rat plasma and only one minor metabolite, N-dealkylated-praligicuat, was present in circulation. The majority of radioactivity was recovered in the bile of BDC rats and in the feces of NBDC rats, with the remainder excreted in urine. Furthermore, no quantifiable parent drug was detected in bile and urine, indicating that the primary route of elimination was hepatic metabolism followed by biliary clearance. Praligicuat was extensively metabolized in rats via oxidative and glucuronidation pathways.

While sGC is widely recognized for its role in NO-cGMP-mediated smooth muscle relaxation, it has also been shown to be expressed and active in many other cell types and tissues throughout the body.¹² Furthermore, dysregulation in the NO-sGC-cGMP signaling pathway has been linked to pathologies in multiple physiological systems.⁴ A key factor in the pharmacological activity of an sGC stimulator is the ability of the molecule to reach the target tissue and achieve adequate residence time at that site of action. In this study, high and sustained levels of praligicuat equivalents were attained in key target tissues of many cardiometabolic diseases, including the liver, kidney, heart, lung, and adipose tissues.

In addition to the anti-inflammatory, antifibrotic, renoprotective, and hepatoprotective effects of praligicuat demonstrated in preclinical models,^{7,13,14} emerging preclinical and clinical data indicate that praligicuat may have favorable effects on metabolic parameters, including cholesterol and insulin resistance.^{9,15,16} These effects are of particular interest since, to our knowledge, they have not been reported for other sGC stimulators in humans and could be accentuated by the extensive tissue distribution of praligicuat.

In conclusion, praligicuat is extensively distributed to tissues and is eliminated by phase 1 and phase 2 metabolic pathways. Given the minor contribution of renal elimination, which was confirmed in the clinic,⁸ praligicuat exposure is not expected to be altered in patients with impaired renal function. The extensive tissue distribution of praligicuat is unique among clinical-stage sGC stimulators, and may make praligicuat particularly well suited for the treatment of cardiometabolic diseases with multiorgan involvement.

ACKNOWLEDGEMENTS

The authors would like to thank Gavrielle Price and Jennifer Chickering for their contributions in reviewing the manuscript.

DISCLOSURES

Peter Germano, Mark G. Currie, and G. Todd Milne are employed by and may own stock/stock options in Cyclerion. Ali R. Banijamali, Andrew E. Carvalho, James D. Wakefield, Timothy C. Barden, Jenny

V. Tobin, Daniel P. Zimmer, Jaime L. Masferrer, and Albert T. Profy may own stock/stock options in Cyclerion.

AUTHORS CONTRIBUTIONS

Participated in research design: Banijamali, Carvalho, Wakefield. Conducted experiments: Banijamali, Carvalho. Contributed new reagents or analytic tools: Barden. Performed data analysis: Banijamali, Carvalho, Wakefield, Germano. Wrote or contributed to the writing of the manuscript: Banijamali, Carvalho, Zimmer, Wakefield, Germano, Tobin, Masferrer, Profy, Milne, Currie.

ORCID

Peter Germano  <https://orcid.org/0000-0002-6766-0885>

REFERENCES

- Ahluwalia A, Foster P, Scotland RS, et al. Antiinflammatory activity of soluble guanylate cyclase: cGMP-dependent down-regulation of P-selectin expression and leukocyte recruitment. *Proc Natl Acad Sci*. 2004;101:1386-1391.
- Sandner P, Zimmer DP, Milne GT, Follmann M, Hobbs A, Stasch JP. Soluble guanylate cyclase stimulators and activators. *Handb Exp Pharmacol*. 2018. https://doi.org/10.1007/164_2018_197
- Derbyshire ER, Marletta MA. Structure and regulation of soluble guanylate cyclase. *Annu Rev Biochem*. 2012;81:533-559.
- Buys ES, Zimmer D, Chickering J, et al. Discovery and development of next generation sGC stimulators with diverse multidimensional pharmacology and broad therapeutic potential. *Nitric Oxide*. 2018;78:72-80.
- Ghofrani HA, Galiè N, Grimminger F, et al. Riociguat for the treatment of pulmonary arterial hypertension. *N Engl J Med*. 2013;369:330-340.
- Ghofrani HA, D'Armini AM, Grimminger F, et al. Riociguat for the treatment of chronic thromboembolic pulmonary hypertension. *N Engl J Med*. 2013;369:319-329.
- Tobin J, Zimmer D, Shea C, et al. Pharmacological characterization of IW-1973, a novel soluble guanylate cyclase stimulator with extensive tissue distribution, anti-hypertensive, anti-inflammatory, and anti-fibrotic effects in preclinical models of disease. *J Pharmacol Exp Ther*. 2018;365:664-675.
- Hanrahan JP, Wakefield JD, Wilson PJ, et al. A randomized, placebo-controlled, multiple-ascending-dose study to assess the safety, tolerability, pharmacokinetics, and pharmacodynamics of the soluble guanylate cyclase stimulator praligicuat in healthy subjects. *Clin Pharmacol Drug Dev*. 2019;8:564-575.
- Hanrahan JP, Wakefield JD, Wilson PJ, et al. 14-Day study of praligicuat, a soluble guanylate cyclase stimulator, in patients with diabetes and hypertension. *Diabetes*. 2018;67:A19.
- Solon E, Lee F. Methods determining phosphor imaging limits of quantitation in whole-body autoradiography rodent tissue distribution studies affect prediction of ¹⁴C human dosimetry. *J Pharmacol Toxicol Methods*. 2002;46:83-91.
- Hop CE, Wang Z, Chen Q, Kwei G. Plasma-pooling methods to increase throughput for in vivo pharmacokinetic screening. *J Pharm Sci*. 1998;87:901-903.
- Budworth J, Meillerais S, Charles I, Powell K. Tissue distribution of the human soluble guanylate cyclases. *Biochem Biophys Res Commun*. 1999;263:696-701.
- Flores-Costa R, Alcaraz-Quiles J, Titos E, et al. The soluble guanylate cyclase stimulator IW-1973 prevents inflammation and fibrosis in experimental non-alcoholic steatohepatitis. *Br J Pharmacol*. 2018;175:953-967.

14. Hall K, Bernier S, Jacobson S, et al. sGC stimulator praliguat suppresses stellate cell fibrotic transformation and inhibits fibrosis and inflammation in models of NASH. *Proc Natl Acad Sci.* 2019;116:11057-11062.
15. Hoffmann LS, Etzrodt J, Willkomm L, et al. Stimulation of soluble guanylyl cyclase protects against obesity by recruiting brown adipose tissue. *Nat Commun.* 2015;6:7235.
16. Schwartzkopf C, Hadcock J, Jones J, Currie M, Milne GT, Masferrer J. Praliguat, a clinical-stage sGC stimulator, improved glucose tolerance and insulin sensitivity and lowered triglycerides in a mouse diet-induced obesity model. *Diabetes.* 2018;67(Supplement 1):1886.

How to cite this article: Banijamali AR, Carvalho AE, Wakefield JD, et al. Pharmacokinetics, mass balance, tissue distribution, metabolism, and excretion of praliguat, a clinical-stage soluble guanylate cyclase stimulator in rats. *Pharmacol Res Perspect.* 2020;e00579. <https://doi.org/10.1002/prp2.579>